The spatial distribution of impact craters on Ryugu

Hirata, Naoyuki ; Morota, Tomokatsu ; Cho, Yuichiro ; Kanamaru, Masanori ; Watanabe, Sei-ichiro ; Sugita, Seiji ; Hirata, Naru ;…

(Citation)
Icarus,338:113527

(Issue Date)
2019-11-05

(Resource Type)
journal article

(Version)
Accepted Manuscript

(URL)
https://hdl.handle.net/20.500.14094/90006493

Title

The spatial distribution of impact craters on Ryugu

Authors

Naoyuki Hirata [a, *], Tomokatsu Morota [b], Yuichiro Cho [b], Masanori Kanamaru [c], Sei-ichiro Watanabe [d], Seiji Sugita [b, e], Naru Hirata [f], Yukio Yamamoto [g], Rina Noguchi [g], Yuri Shimaki [g], Eri Tatsumi [b, h], Kazuo Yoshioka [i], Hirotaka Sawada [g], Yasuhiro Yokota [g, j], Naoya Sakatani [g], Masahiko Hayakawa [g], Moe Matsuoka [g], Rie Honda [j], Shingo Kameda [k], Manabu Yamada [e], Toru Kouyama [l], Hidehiko Suzuki [m], Chikatoshi Honda [f], Kazunori Ogawa [a], Yuichi Tsuda [g], Makoto Yoshikawa [g], Takanao Saiki [g], Satoshi Tanaka [g], Fuyuto Terui [g], Satoru Nakazawa [g], Shota Kikuchi [g], Tomohiro Yamaguchi [g, n], Naoko Ogawa [g], Go Ono [o], Yuya Mimasu [g], Kent Yoshikawa [o], Tadateru Takahashi [g], Yuto Takei [g], Atsushi Fujii [g], Hiroshi Takeuchi [g], Tatsuaki Okada [g], Kei Shirai [g], Yu-ichi Iijima [p].

* Corresponding Author E-mail address: hirata@tiger.kobe-u.ac.jp

Authors' affiliation

[a] Department of Planetology, Kobe University, Kobe 657-8501, Japan.

[b] Graduate School of Science, University of Tokyo, Tokyo 113-0033, Japan.

[c] Department of Earth and Space Science, Osaka University, Osaka 560-0043, Japan.

[d] Graduate School of Environmental Studies, Nagoya University, Nagoya 464–8601, Japan.

[e] Planetary Exploration Res. Center, Chiba Institute of Technology, Narashino 275-0016, Japan.

[f] University of Aizu, Aizu-Wakamatsu 965-8580, Japan.

[g] Institute of Space and Astronautical Science, JAXA, Sagamihara 252-5210, Japan.

[h] Instituto de Astrofisica de Canarias, University of La Laguna, Tenerife, E38205, Spain.

[i] Graduate School of Frontier Sciences, University of Tokyo, Kashiwa 277-8561, Japan.

[j] Kochi University, Kochi 780-8520, Japan.

[k] College of Science, Rikkyo University, Tokyo 171-8501, Japan.

[l] National Institute of Advanced Industrial Science and Technology, Tokyo 135-0064, Japan.

[m] Meiji University, Kanagawa 214-8571, Japan.

[n] Mitsubishi Electric Corporation, Kamakura 247-8520, Japan.

[o] Research and Development Directorate, JAXA, Sagamihara 252-5210, Japan.

[p] Deceased

Proposed Running Head: Craters on Ryugu

Editorial Correspondence to:

Dr. Naoyuki Hirata

Kobe University, Rokkodai 1-1 657-8501

Tel/Fax +81-7-8803-6566

Key Words

Asteroid

Impact processes

Geological processes

Highlights

- We examined the spatial distribution of impact craters on Ryugu
- We completed a global impact crater catalogue of Ryugu (D>20 m)
- Crater density variations cannot be explained by the randomness of cratering
- More craters are seen at lower latitudes and less at higher latitudes
- There are fewer craters in the western bulge and more around the meridian

Abstract

Asteroid 162173 Ryugu has numerous craters. The initial measurement of impact craters on Ryugu, by Sugita et al. (2019), is based on Hayabusa2 ONC images obtained during the first month after the arrival of Hayabusa2 in June 2018. Utilizing new images taken until February 2019, we constructed a global impact crater catalogue of Ryugu, which includes all craters larger than 20 m in diameter on the surface of Ryugu. As a result, we identified 77 craters on the surface of Ryugu. Ryugu shows variation in crater density which cannot be explained by the randomness of cratering; there are more craters at lower latitudes and fewer at higher latitudes, and fewer craters in the western bulge (160°E – 290°E) than in the region around the meridian (300°E – 30°E). This variation implies a complicated geologic history for Ryugu. It seems that the variation in crater density indicates that

the equatorial ridge located in the western hemisphere is relatively young, while that located in the eastern hemisphere is a fossil structure formed during the short rotational period in the distant past.

1. Introduction

Ryugu is a top-shaped asteroid with a mean radius of 448 m and a rotational obliquity of 8 degrees (Watanabe et al., 2019). Since JAXA's Hayabusa2 spacecraft arrived at asteroid 162173, Ryugu, on June 27, 2018, the onboard optical navigation cameras (ONC) have obtained numerous images of Ryugu and revealed many surface features, including abundant impact craters (Sugita et al., 2019). This cratering suggests that a major process in the formation of the surface of Ryugu has been via impacts from other bodies. The low bulk density of Ryugu implies that the asteroid is composed of fragments that probably resulted from catastrophic disruption (Watanabe et al., 2019). The initial report of impact craters on Ryugu (Sugita et al. 2019) was produced via the utilization of ONC images from July to August 1, 2018, which identified approximately 30 impact craters from the limited coverage of Ryugu. The surface crater retention age was estimated to be in the order of 10^7 or 10^8 years, based on the number density of craters of 100 – 200 m in diameter (D). In addition, Sugita et al. (2019) reported that the crater size-frequency distribution (CSFD) of Ryugu shows a lack of small craters ($D < 100$ m), which indicates that the average resurfacing of the top ~1-meter layer on Ryugu takes less than 10^6 years. Ryugu has a west/east dichotomy (Sugita et al. 2019); its western side, the so-called western bulge, (160°E – 290°E), has a high albedo, a low number density of large boulders, is topographically high, and has a bluish color as compared to the eastern side. The equatorial ridge located in the eastern hemisphere is slightly offset towards the south.

The main purpose of this paper is (i) to present the basic information (the location and size of each craters), which is not listed in the initial report by Sugita et al. (2019), (ii) to accomplish a global catalogue of all the craters ($D \geq 10$ - 20 m), utilizing additional images acquired after the publication by Sugita et al. (2019) which have allowed the investigation of craters over the entire surface of Ryugu, (iii) to investigate the statistical significance of the spatial distribution of the impact craters. Note that we do not discuss the crater size-frequency distribution or the depletion and retention time of small craters, as these topics will be included in Morota et al. (in preparation).

2. DATA and Method

2.1. Crater counting

This study utilized 340 ONC images for crater counting (Table 1): (i) 96 images obtained in July 20 2018 with a ground resolution of 0.72 m/pixel providing global coverage excluding the polar regions > 70 degrees, (ii) 85 images obtained on August 1 2018 with a resolution of 0.69-0.55 m/pixel, providing regional coverage of low latitudes < 40 degrees, (iii) 11 images obtained on October 4 2018 with a resolution of 0.32 m/pixel, providing coverage of the north pole, (iv) 18 images on October 30 2018 with a resolution of 0.62 m/pixel providing coverage of the north and south poles (v) 26 images obtained on February 28 2019 with a resolution of 0.67 m/pixel providing coverage of the north and south poles, (vi) 52 images obtained on August 23 2018 with a resolution of 2.6 m/pixel providing coverage of the

127 south pole, (vii) 52 images obtained on January 24 2019 with a resolution of
128 2.1 m/pixel providing coverage of the north pole. Because the Hayabusa 2
129 spacecraft is generally remaining in the same position above the sub-Earth
130 point of the asteroid's surface and the rotational obliquity of Ryugu is small,
131 the emission angles of the images (i)-(v) are large for polar regions. The
132 low-emission images of Ryugu's polar regions, (vi) and (vii), were obtained at
133 a position distant from the equatorial plane. All of the impact craters were
134 identified from these ONC images. These ONC images will be freely
135 available at the end of 2020. Craters with diameters larger than 10-20 m
136 could be clearly identified as these images had a resolution of at least 10
137 pixels (though they had a resolution of less than 10 pixels in the case of the
138 image subset (iv)). We note that the choice of the minimum pixel number for
139 reliable crater identification requires care; it varies substantially depending
140 on imaging conditions, such as solar incidence angle. Also, stereo pair images
141 greatly improve the robustness of crater identification. Because the
142 Hayabusa2 ONC image dataset used in this study covers almost entire
143 surface of Ryugu with multiple imaging and large solar incidence angles, 10
144 pixel is sufficient for identifying craters on Ryugu. The images enabled us to
145 identify all impact craters exceeding 10 – 20 meters diameter over the entire
146 surface of Ryugu. Therefore, to ensure that crater counting was not affected
147 by image resolution, D = 20 m was set as the minimum diameter threshold.
148 We identified all circular or quasi-circular depressions as craters for
149 this study. This included cases where the circular depression lacked a raised
150 rim. However, we did not regard circular features without topographic

depressions as craters. Features such as topographic depression or rims were judged from (i) the shape model of Ryugu (Watanabe et al. 2019), (ii) visual observation using stereo pairs and (iii) visual observation based on shading of images at low sun. Based on these criteria, we classified all the candidate craters into types: I-IV (as summarized in Table 2). We judged those classified as types I-III to be distinct crater (Nos. 1- 77 in Figure 1), and classification IV to be less-distinct crater. For this study, we assumed that type IV phenomena are not craters (Nos. 78-86 in Figure 1), and therefore these were not included in crater density and statistical analysis. Nonetheless, many craters were more or less degraded and infilled with regolith or boulders and often lacked distinct shape, and this interpretation was therefore often ambiguous.

To measure the size, latitude, and longitude of each crater we utilized the Small Body Mapping Tool (Kahn et al., 2011), a global image mosaic map of Ryugu, and a shape model of Ryugu. The global image mosaic map was built from the ONC images, and the shape model was derived from Watanabe et al. (2019). The Small Body Mapping Tool was used to measure the diameters and locations of the craters for the study. This software enabled measurement of the centers and diameters of craters based on three points selected along the crater rim from a global mosaic map rendered onto the shape model.

A fairly accurate surface area is required to obtain the number density of the craters. In the case of an irregular-shaped asteroid, the definition of the surface area is complicated. When defining it from a shape

model, the surface area increases infinitely as the resolution of the shape model increases. To simplify, the surface area was not determined as the total area of the surface polygons composing the shape model, but was instead calculated as the surface of a sphere with a radius of 448 m. The total surface area of Ryugu was thus calculated to be 2.5 km^2. We note that the shape model of Ryugu (SHAPE_SFM_200k_v20180804.obj), which describes Ryugu as 196608 plates, has the surface area of 2.77 km^2.

2.2. The statistical analysis of the spatial distribution

A statistical test was then performed to evaluate the significance of variations in the crater density. The nearest-neighbor analysis was thus used to discover whether the variation can be explained merely by randomness, following the methodology of Squyres et al. (1997). The distance between each point (i.e. the center of a crater) and its nearest neighboring point (i.e. the center of the nearest neighbor crater) was determined and averaged, and the mean distance observed was compared with the mean distance expected under random distribution. If the observed value was significantly smaller (greater) than the expected value, the distribution was considered to be significantly clustered (ordered) and not random. This method has been applied to evaluate the distribution of craters on various solar system objects. Phillips et al. (1992) found that, although Venus has a variation in crater density, the variation cannot be distinguished from a completely random distribution; therefore, the variation can be explained by the randomness of the crater production on that planet. Squyres et al. (1997) found that the crater distributions on Callisto and Rhea are not random but are

199 significantly ordered. The spatial distribution of observed craters in heavily
200 cratered terrain transition from random to ordered because craters that form
201 in sparse areas obliterate the relatively few existing craters, filling in the
202 spaces, whereas craters that form in areas of existing crater clustering
203 obliterate the existing craters and reduce the clustering (Lissauer et al.
204 1988; Squyres et al. 1997). Moreover, partial resurfacing such as lava flow or
205 the mass-movement of rock tends to create clustered crater distribution.
206 Following Squyres et al. (1997), the Z value was determined to assess
207 the degree by which the value of the observed mean distance (d_{obs}) deviates
208 from randomness:
209 $$Z \equiv \frac{d_{obs} - d_{exp}}{\sigma} \quad , (1)$$
210 where d_{exp} is the expected mean distance when the distribution is completely
211 random and σ is the standard deviation of d_{exp}. A positive Z value indicates
212 that the distribution of points is ordered, a negative Z value indicates that it
213 is more clustered, and a value of Z close to 0 indicates that the distribution
214 cannot be distinguished from random. A value for Z was obtained for the
215 distribution of all craters that exceeded a given diameter. The Z-statistic was
216 not calculated in cases where the number of craters was lower than $n = 2$.
217 The observed distance between two points was determined on the basis of
218 the great-circle distance between the two points on the unit sphere, although
219 the shape of Ryugu is not spherical. Values for d_{exp} and σ were calculated
220 numerically using the Monte Carlo simulation, following Hirata (2017). This
221 study assumed that (1) n points were produced on the unit sphere, (2) these
222 points were randomly generated because the impactors were assumed to

have come from all directions, (3) the mean distance to the nearest neighbor (d_i in i^{th} trial) was measured using the average of the lengths defined by the great-circle distance between two points, (4) based on these three assumptions, 10000 trials were performed, and (5) the average and deviation of d_i (i = 1,2,3, …10000) were obtained as d_{exp} and σ, respectively.

3. Results

On the surface of Ryugu, 77 craters were identified (Fig. 1); the diameters and locations of these craters are listed in Table 3. Figure 2 shows the global distribution of craters that are bordered with rims as lines on the global mosaic map projected in a simple cylindrical projection. We again confirmed a lack of small craters (20 m < D < 100 m) relative to the number of large craters, as has also been found on other small asteroids such as Itokawa, Eros, and Bennu (Thomas and Robinson, 2005; Michel et al. 2009; Walsh et al. 2019). The largest crater on Ryugu is Urashima, at 290 m in diameter, which is equivalent to 32% of the diameter of Ryugu. The second and third largest craters are Cendrillon (224 m) and Kolobok (221 m), respectively. Only these three craters exceed 200 meters in diameter. The average crater density over Ryugu is 4.4 craters/km^2 for D ≥ 100 m and 25.0 craters/km^2 for D ≥ 20 m.

The distribution of craters on Ryugu is variable, with differences in crater density depending on longitude and latitude (Fig 3a, b). The Z value (Fig. 3c) suggests that the craters on Ryugu are spatially distributed in clusters, in a statistically significant manner. Therefore, the spatial

distribution of craters on Ryugu cannot be explained by the randomness of cratering itself. There are more craters at lower latitudes and fewer craters at higher latitudes (Fig. 3b). Polar regions of greater than 40 degrees latitude have only a few craters. There are more craters around the meridian (300°E-30°E), and fewer at the western bulge (160°E – 290°E). Because of this we termed the region between 300°E-30°E and 40°S-40°N the cratered terrain. The crater density in this region is 57.3 craters/km^2 ($D \geq 20$ m), twice the global average. However, as shown in Fig 3a, the crater density of the western bulge is roughly half the global average. Although less-cratered terrain is often found both surrounding and on the inside of large craters such as Shoemaker crater on Eros (Robinson et al. 2002), we could not identify any landform that could be associated with a putative large crater at either the polar regions or the western bulge of Ryugu.

Ryugu has 11 craters ($D \geq 100$ m), of which 5 cut the crest of the equatorial ridge, Ryujin Dorsum. Note that we concluded that it is unlikely that some of the impact craters found on this ridge did not originate from impacts (i.e., the ridge is a landform made by another mechanism such as mass-movement). This is because the large craters cutting across the ridge (No. 1, 3, 4, 6, 8 in Fig. 1) are all clear and circular bowl-shaped depressions and appear to be distinct impact craters, as discussed by Sugita et al. (2019). We therefore performed a statistical test to evaluate the statistical significance of the concentration of craters on the equatorial ridge, Ryujin Dorsum. Using the Monte Carlo method, we estimated the number of craters expected across the equator under random distribution. In detail: (1) the 11

craters exceeding diameters of 100 m, are placed at random points on a sphere with a radius of 448 m using spherical uniform random numbers, (2) the number of craters across the equator is counted, and (3) the average value of the number and its dispersion are obtained from 1000 trials. Results indicate that the expected number of large craters across the equator under random distribution is 2.1 with a dispersion of 1.3. We therefore concluded that the number of observed craters found on the equator (5 craters) was greater than that expected randomly.

4. Discussion

Possible explanations for the longitudinal variation in crater density are: (i) resurfacing from processes such as seismic shaking is inert in the cratered terrain and is more active in the western bulge, (ii) differences in the physical terrain inhibit the formation of an impact crater (e.g., Güttler et al. (2012) proposed an armoring effect owing to the presence of boulders), and (iii) the cratered terrain around the meridian (300°E -30°E) is geologically old, while the formation of the western bulge was relatively recent. Seismic shaking or armoring effects, as in (i) and (ii), should theoretically be more effective for smaller craters; however, even large craters on Ryugu show longitudinal variation which indicates that (i) and (ii) are unlikely. We propose that (iii) is the most likely scenario. This is because the western bulge is a geologically distinct terrain, as mentioned in Section 1. The western bulge is proposed to have been caused by the deformation of Ryugu, via a process that occurred on only the western side of the asteroid

during a short rotational period of Ryugu in the past, while the eastern hemisphere was left structurally intact (Hirabayashi et al. 2019). On the other hand, Scheeres (2015) proposed that regolith landslides occur on the surface of rapidly spinning asteroids, so the occurrence of such a landslide from the polar regions toward the western hemisphere could be taken into consideration as an alternative explanation for the formation of the western bulge. In addition, such a landslide could be responsible for the latitude variation in crater density (i.e. relatively less-cratered polar regions). In both cases, the crater density of the western bulge represents the timing of the short rotational period of Ryugu, while the cratered terrain around the meridian was already an old surface when the western bulge formed. Probably, the equatorial ridge located in the eastern hemisphere is a fossil structure formed during the short rotational period in the distant past. The ridge that is slightly offset towards the south may indicate a polar shift of Ryugu in the past.

5. Conclusion

We have identified 77 craters on the surface of Ryugu. The spatial distribution of the craters on Ryugu is not random, with variations in crater density that can be linked to latitude and longitude; more craters are seen at lower latitudes than at higher latitudes, and there are more craters in the region around the meridian than in the western bulge. The longitudinal variation in crater density could be a possible result of the formation of the western bulge, which is thought to have formed later than the rest of the

asteroid due to its lower proportion of craters. The equatorial ridge located in the eastern hemisphere would be a fossil structure formed during the short rotational period in the distant past.

Acknowledgements

This study was supported by the JSPS International Planetary Network. Images obtained by Hayabusa2 will be freely available via Data ARchives and Transmission System (DARTS) at ISAS/JAXA at the end of 2020 (https://www.darts.isas.jaxa.jp/index.html.en). The shape model of Ryugu has already been released in DARTS. The Small Bodies Mapping Tool has been released at http://sbmt.jhuapl.edu/index.html.

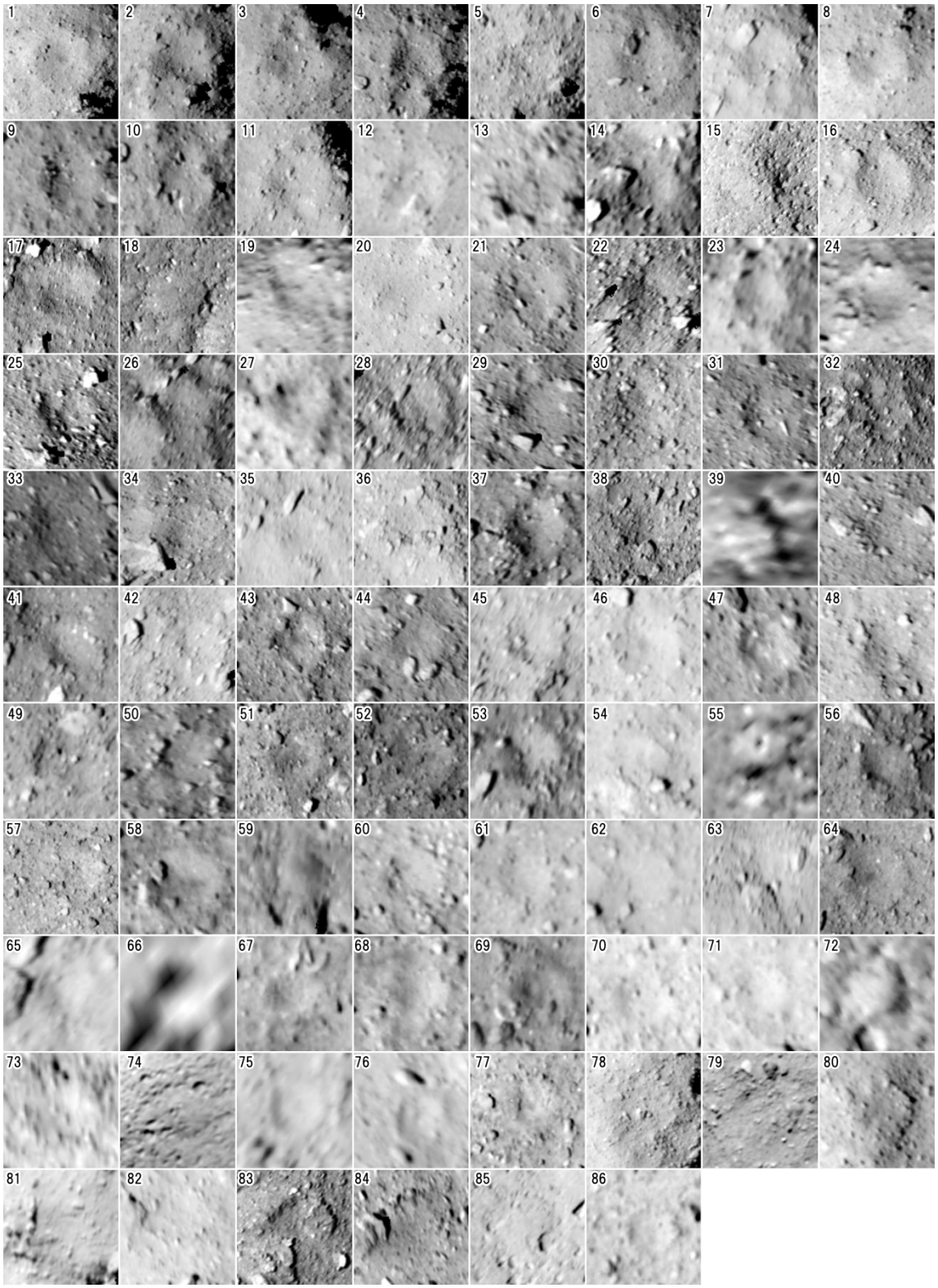

Figure 1. Candidate craters that were identified. Numbers correspond to those in Table 3.

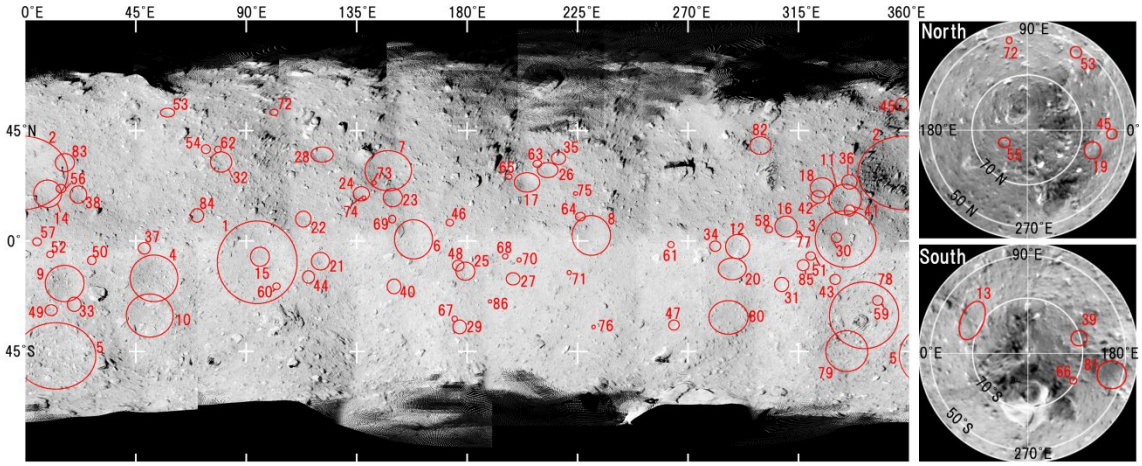

Figure 2. The distribution of craters on Ryugu. Red lines roughly outline the rim of craters. On the left is a simple cylindrical projection mosaic map derived from the July 20, 2018 images. On the right is the azimuthal equidistant projection maps centered in the north (top) and south poles (bottom) derived from January 24, 2019 and August 23, 2018. Numbers correspond to Figure 1 and Table 3.

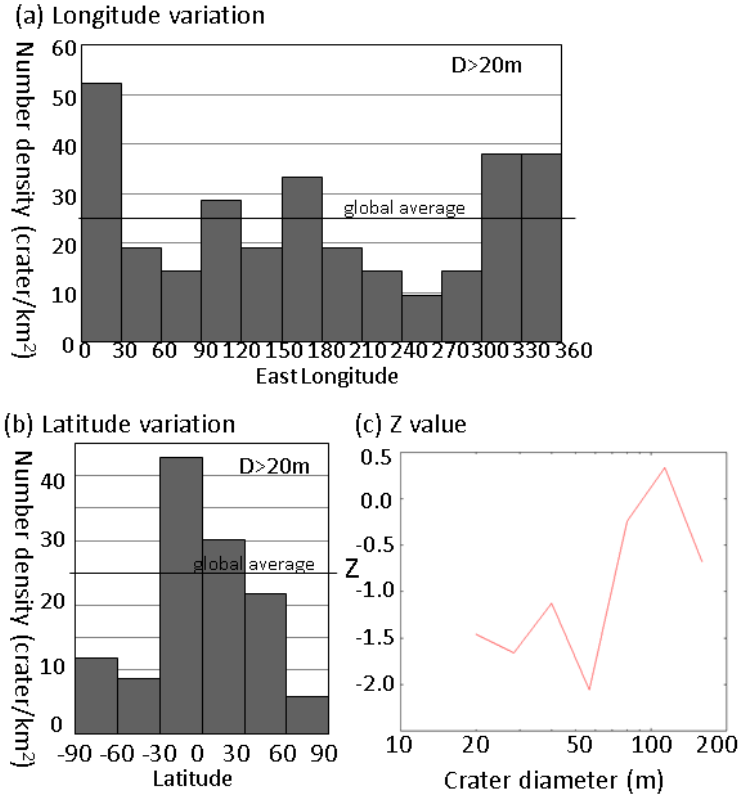

344 **Figure 3. (a)** The longitudinal variation in crater density (D ≥ 20 m). **(b)** The
345 latitudinal variation in crater density (D ≥ 20 m). **(c)** The Z value for spatial
346 distribution on Ryugu.

347

348 **Table 1. Images utilized in this work.**

	Date	Num.	Resolution	Note
(i)	Jul. 20 2018	96	0.72 m/px	Low latitude < 70 degree
(ii)	Aug.1 2018	85	0.69-0.55 m/px	Low latitude < 40 degree
(iii)	Oct. 4 2018	11	0.32 m/px	North pole
(iv)	Oct. 30 2018	18	0.62 m/px	North and South poles
(v)	Feb. 28 2019	26	0.67 m/px	North and South poles
(vi)	Aug. 23 2018	52	2.6 m/px	South pole at small emission

(vii)	Jan. 24 2019	52	2.1 m/px	North pole at small emission

349

350 **Table 2.** Classification in this study.

Classification	Characteristic	Our Judge
I	Circular depression with rim	Crater
II	Circular depression without rim	Crater
III	Quasi-circular depression	Crater
IV	Quasi-circular features	Not crater

351

352 **Table 3.** Impact craters on Ryugu

#*1	Lat.	Lon. (°E)	D (m)	CL*2
Classification I-III				
1	-7.19	92.99	290	I
2	28.34	353.68	224	II
3	-0.70	330.28	221	II
4	-14.83	51.20	183	I
5	-50.56	9.84	173	III
6	0.42	157.84	154	II
7	30.37	145.99	145	II
8	3.24	229.95	142	I
9	-17.19	14.29	133	II
10	-31.50	47.26	131	I
11	17.02	332.23	100	I
12	-1.88	289.49	90.2	II
13	-63.73	24.45	85.0	III
14	16.90	6.44	79.0	III
15	-4.54	95.52	78.9	III
16	6.01	308.75	77.1	I
17	23.70	205.33	76.2	II
18	20.86	322.68	73.9	II
19	57.73	342.98	73.3	II

20	-11.64	287.71	69.0	III
21	-8.44	119.53	69.0	I
22	8.28	111.52	65.8	III
23	18.59	149.73	65.8	II
24	19.65	136.94	62.1	II
25	-12.18	179.11	61.0	II
26	28.48	213.16	58.2	II
27	-16.28	199.13	53.6	II
28	36.81	121.83	52.2	III
29	-36.18	176.65	51.3	III
30	-0.07	329.24	51.3	II
31	-17.20	307.19	48.8	II
32	33.09	81.45	48.4	III
33	-26.28	17.83	46.6	II
34	-1.87	279.89	44.2	II
35	33.50	217.25	44.1	III
36	24.37	335.50	43.1	III
37	-3.08	47.02	42.7	I
38	18.62	20.92	42.5	III
39	-69.03	170.39	41.7	III
40	-19.49	150.94	41.4	III
41	11.91	334.53	39.9	I
42	17.52	323.27	39.7	II
43	-15.38	328.28	37.2	II
44	-14.87	115.35	36.5	II
45	55.75	357.50	36.0	II
46	7.79	173.00	34.6	I
47	-34.51	263.82	34.4	I
48	-10.68	176.31	32.0	II
49	-28.57	9.83	30.6	III
50	-7.92	26.75	29.3	III
51	-6.30	319.67	28.1	III
52	-5.81	9.76	27.6	III
53	52.36	57.31	27.5	II
54	37.10	73.44	26.5	III
55	79.00	209.00	26.0	II

56	21.44	13.71	25.3	III
57	-0.89	4.52	24.4	III
58	4.61	301.74	23.6	I
59	-24.00	346.55	21.7	III
60	-19.26	102.14	21.5	III
61	-2.08	263.10	21.0	II
62	37.02	78.22	20.9	III
63	31.21	208.26	20.2	III
64	8.40	225.72	17.2	I
65	25.81	196.97	16.2	II
66	-69.00	211.00	16.0	II
67	-31.59	174.66	14.5	II
68	-6.96	195.40	14.4	III
69	9.65	149.10	14.0	I
70	-8.37	201.10	14.0	II
71	-12.89	221.27	13.9	II
72	52.43	100.93	12.6	II
73	23.18	141.89	12.5	II
74	17.15	137.76	11.4	II
75	19.01	224.05	11.2	II
76	-35.88	231.29	10.5	II
77	3.40	314.61	10.0	II
		Classification IV		
78	-31.21	341.74	223	IV
79	-45.92	334.99	133	IV
80	-30.64	284.23	112	IV
81	-58.37	198.43	112	IV
82	38.21	298.88	55.8	IV
83	31.87	15.43	53.0	IV
84	10.26	69.87	46.7	IV
85	-10.59	316.99	35.0	IV
86	-25.36	189.21	11.4	IV

[*1] Number in descending order of diameter. Ryugu has 7 named craters: Urashima (No.1), Cendrillon (No.2), Kolobok (No.3), Momotaro (No.4), Kintaro (No. 6), Brabo (No. 8), and Kibidango (No.10).

356 [*2] Classification shown in Table 2.

357

358 **References**

359 Güttler, C., N. Hirata, and A.M. Nakamura (2012) Cratering experiments on
360 the self armoring of coarse-grained granular targets. *Icarus* 220(2),
361 1040-1049.

362 Hirabayashi et al. (2019), The Western Bulge of 162173 Ryugu Formed as a
363 Result of a Rotationally Driven Deformation Process. *The*
364 *Astrophysical Journal Letters* 874, Number 1.

365 Hirata N. (2017) Spatial distribution of impact craters on Deimos. *Icarus* 288,
366 69-77.

367 Kahn, E. G., O. S. Barnouin, D. L. Buczkowski, C. M. Ernst, N. Izenberg, S.
368 Murchie and L. M. Prockter. (2011) A Tool for the Visualization of
369 Small Body Data. In *42nd Lunar and Planetary Science Conference*,
370 Abstract #1618. Houston: Lunar and Planetary Institute.

371 Lissauer, J. J., S. W. Squyres, and W. K. Hartmann (1988), Bombardment
372 History of the Saturn System, Journal of Geophysical Research: Solid
373 Earth, 93(B11), 13776-13804.

374 Michel, P., D. P. O'Brien, S. Abe, and N. Hirata, (2009) Itokawa's cratering
375 record as observed by Hayabusa: implications for its age and
376 collisional history. *Icarus* 200, 503–513.

377 Phillips, R. J., R. F. Raubertas, R. E. Arvidson, I. C. Sarkar, R. R. Herrick, N.
378 Izenberg and R. E. Grimm (1992) Impact craters and Venus
379 resurfacing history. *Journal of Geophysical Research: Planets* 97,

15923-15948.

Robinson, M. S., P. C. Thomas, J. Veverka, S. L. Murchie, and B. B. Wilcox (2002) The geology of 433 Eros. *Meteoritics & Planetary Science* 37(12), 1651-1684.

Scheeres, D.J., (2015) Landslides and Mass shedding on spinning spheroidal asteroids. *Icarus* 247, 1-17.

Squyres, S. W., C. Howell, M. C. Liu and J. J. Lissauer (1997) Investigation of Crater "Saturation" Using Spatial Statistics. *Icarus* 125, 67-82.

Sugita, S. et al. (2019) The geomorphology, color, and thermal properties of Ryugu: Implications for parent-body processes. *Science* 364, 272-275.

Thomas, P. C. and M.S. Robinson, (2005) Seismic resurfacing by a single impact on the asteroid 433 Eros. *Nature* 436, 366–369.

Walsh, K. J. et al. (2019), Craters, boulders and regolith of (101955) Bennu indicative of an old and dynamic surface. *Nature Geoscience* 12, 242–246.

Watanabe S. et al. (2019) Hayabusa2 arrives at the carbonaceous asteroid 162173 Ryugu—A spinning top–shaped rubble pile. *Science* 364, 268-272.